Liquid Crystals
Publication details, including instructions for authors and subscription information:
http://www.informaworld.com/smpp/title~content=t713926090

A bent-core dopant-induced smectic A* twist state

P. Archer[a]; I. Dierking[a]
[a] School of Physics and Astronomy, The University of Manchester, Schuster Building, Manchester M13 9PL, UK

To cite this Article Archer, P. and Dierking, I.(2006) 'A bent-core dopant-induced smectic A* twist state', Liquid Crystals, 33: 3, 257 — 265
To link to this Article: DOI: 10.1080/02678290600583185
URL: http://dx.doi.org/10.1080/02678290600583185

Liquid Crystals, Vol. 33, No. 3, March 2006, 257–265

Taylor & Francis
Taylor & Francis Group

A bent-core dopant-induced smectic A* twist state†

P. ARCHER and I. DIERKING*

School of Physics and Astronomy, The University of Manchester, Schuster Building, Oxford Road, Manchester M13 9PL, UK

(*Received 20 July 2005; in final form 8 December 2005; accepted 15 December 2005*)

The phase behaviour of a commercial calamitic ferroelectric liquid crystal mixture, doped with different mesogenic and non-mesogenic bent-core molecules was investigated through polarising microscopy, optical measurements and quenched growth. A twisted smectic structure, similar but not equivalent to a twist grain boundary (TGB) phase, and absent in the neat FLC mixture, was verified. The twisted smectic state can only be observed on cooling and its stability depends on the rate of temperature decrease, which indicates a kinetically governed behaviour. Further, the growth dynamics of the low temperature uniform SmA* bookshelf structure is dominated by viscosity instead of free energy density, as would be expected for a true thermodynamic phase transition. The investigations signify the chiral induction capability of achiral, bent-core dopant molecules and we believe that the observed behaviour represents the onset of TGB formation at very large pitch. It can thus give valuable information for the fundamental physical understanding of twist grain boundary phase formation.

1. Introduction

From basic elasticity considerations, twist is incompatible with the layered structure of a smectic A phase due to the incompressibility of smectic layers [1]. Nevertheless, nature has found a way to avoid such rigid constraints by the introduction of screw dislocations arrays between blocks of the ordinary SmA phase. Such phases are known as twist grain boundary (TGB) phases [2–7] (see also [8], [9] and references therein), which represent frustrated phases resulting from the competition between chirality and smectic layer formation. TGB phases are generally observed over only narrow temperature intervals, because the introduction of defects is only accomplished at the cost of free energy. Their basic key structural features are: (i) a layered structure, (ii) a helical superstructure and (iii) a helix axis parallel to the smectic layer plane.

TGB phases are often observed in highly chiral single component mesogens, but have also been reported to be induced in liquid crystal mixtures [10–14] and liquid crystals doped with chiral materials, which may be mesogenic or non-mesogenic by themselves [15–17]. Twist grain boundary phases are fluid smectic phases, i.e. they exhibit one-dimensional positional order. Their textural appearance between crossed polarizers often bears strong similarities to the cholesteric phase; preparation under planar boundary conditions generally results in a Grandjean-like texture, while homeotropic anchoring leads to typical TGB filaments [9, 18]. Nevertheless, subtle differences in textural appearance can be observed between the cholesteric and the TGB phases, especially when the pitch of the helical superstructure is large, i.e. several micrometers as compared with hundreds of nanometers.

It has been attempted to induce TGB-like structures by mechanical twisting of an achiral SmA phase [19], but unambiguous conclusions could not be drawn at that time. In this paper we report an unusual SmA* twist state, induced by doping a liquid crystal with the recently discovered 'banana' or bent-core mesogens [20, 21]. The latter have lately attracted considerable interest due to their polar properties arising from achiral molecules [22], but only few reports towards their use as dopant molecules have been published to date. These have shown induced antiferroelectric phases in ferroelectric hosts [23, 24] and enhanced chirality by addition of achiral bent-core molecules to chiral hosts [25–27].

2. Experimental

The liquid crystal host used throughout this study is a commercial ferroelectric liquid crystal (FLC) mixture, FELIX M4851-050 from Clariant, Wiesbaden,

*Corresponding author. Email: ingo.dierking@manchester.ac.uk

†This paper is dedicated to Sven T. Lagerwall on the occasion of his 70th birthday

Liquid Crystals
ISSN 0267-8292 print/ISSN 1366-5855 online © 2006 Taylor & Francis
http://www.tandf.co.uk/journals
DOI: 10.1080/02678290600583185

Germany, with phase sequence I 78 N* 71 SmA* 67 SmC* −20 Cr (all temperatures in °C). Two bent-core shaped molecules were added to the host at varying, but small, concentrations (*c.*<3% by weight):

(i) non-mesogenic 859

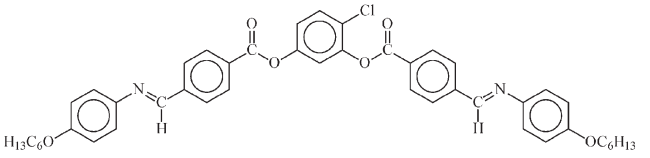

with a phase sequence of I. 138 Cr, and

(ii) mesogenic HXVIII

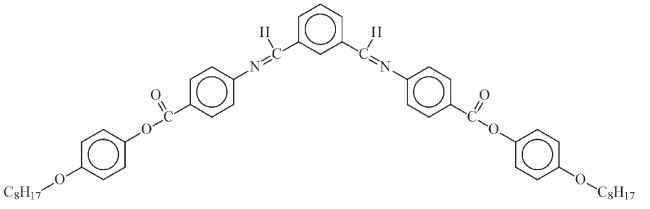

with a phase sequence of I 149 B2 148 B4 121 Cr, as determined by polarizing microscopy. Doping at concentrations larger than 2.5% resulted in phase separation between the host and the dopant. The two dopant molecules not only vary with respect to their liquid crystalline behaviour, but also in their bend-angles, which are 144° for '859' and 119° for 'HXVIII', as determined by molecular modelling with HyperChem 7.5.

For verification of the chiral induction capability of the achiral 'banana' dopants, additional experiments were carried out by doping the FLC host with a commercial chiral dopant, R1011, from Merck, Darmstadt, Germany:

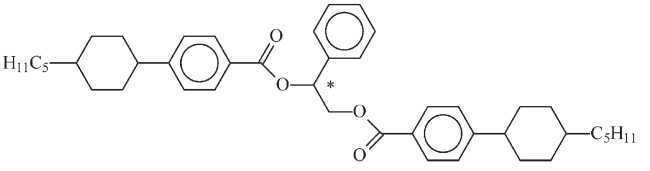

Materials were filled into sandwich cells of gaps between 4 and 25 μm, coated with alignment layers promoting both planar (Nylon 6/6) as well as homeotropic (OTMS, octadecyltrimethoxysilane) boundary conditions. Cell filling took place by capillary action in the isotropic phase. Texture and twist state stability analysis was carried out by polarizing microscopy (Nikon Optiphot-Pol) equipped with a Linkham TMS91 hotstage for relative temperature control to better than 0.1 K and image acquisition (JVC model KY-F1030U). Optical transmission as a function of cell rotation angle between crossed polarizers was followed by use of a high resolution photo-detector in conjunction with a digital storage oscilloscope (Tektronix TDS 3014B).

This experimental set-up was also employed for the reported growth studies, allowing image acquisition at a resolution of 1280 by 960 pixels, corresponding to 520 μm by 390 μm, at a time resolution of 1 s. The growth dynamics of the SmA* phase from the twisted structure was subsequently obtained by digital image analysis employing software ImageTool 3.0, developed at the University of Texas Health Science Centre, San Antonio, USA. Samples were quenched from the cholesteric phase across the twisted state into the temperature regime of the SmA* phase at a rate of $3\,\mathrm{K\,min^{-1}}$. This rate represented the best compromise between temperature control and achievable quench depth, although qualitatively equivalent growth behaviour was also obtained for different cooling rates. The quench depth ΔT referred to below denotes the temperature difference between the transition temperature from the twist state to the SmA* phase and the actual temperature. In the quench experiments the SmA* phase was the equilibrium phase growing at isothermal conditions from the metastable environment of the high temperature smectic twist state.

3. Results and discussion

Doping of the commercial ferroelectric mixture with bent-core shaped molecules of mesogenic as well as non-mesogenic nature, resulted in the observation of an unusual twist state, which is clearly absent in neat FELIX M4851-050. Figure 1 depicts the respective phase diagrams at a cooling rate of $2\,\mathrm{K\,min^{-1}}$ (15 μm cell) for the '859' and HXVIII dopants in parts (*a*) and (*b*), respectively. Transition temperatures are found to decrease with increasing dopant concentration in all cases, and a new twist state emerges between the cholesteric (N*) and smectic A* (SmA*) phase, even for rather low bent-core molecule concentrations of 0.5 wt %. At equal concentrations the smectic twist state exhibits a larger range of stability for the HXVIII dopant as compared with 859. It thus appears that a larger molecular bend of the dopant molecule enhances the stability of the observed smectic twist state.

The chiral host being a multi-component mixture, biphasic regions are expected to occur. Indeed, the latter can clearly be observed in the neat host at the isotropic to cholesteric transition. Nevertheless, we can observe no indication of a two-phase region of any appreciable width (>0.1 K) at the cholesteric to smectic A* transition. In the neat host we do not observe the coexistence of the N* and the SmA* phase, nor do we

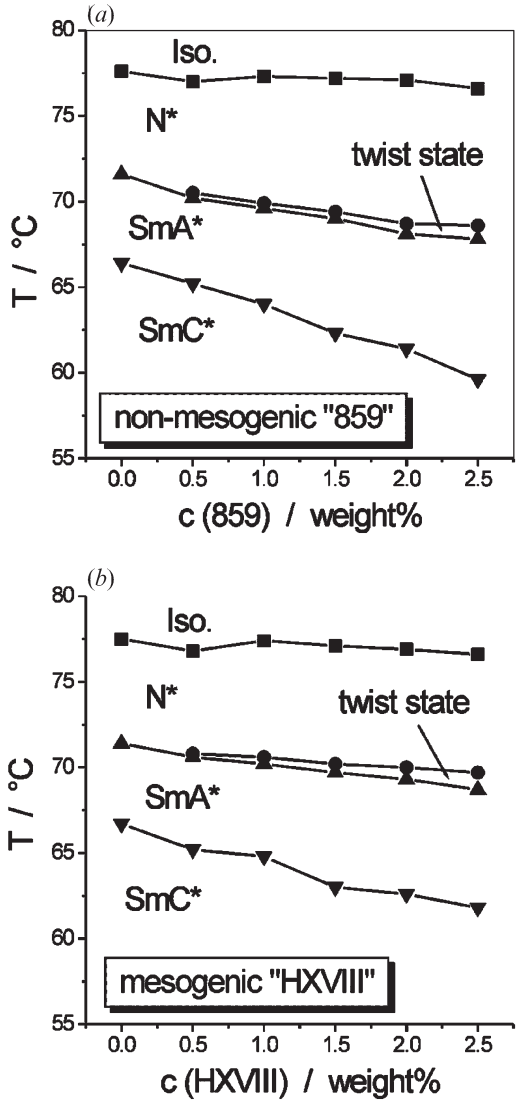

Figure 1. Phase diagrams of (*a*) '859' and (*b*) 'HXVIII' bent-core doped FELIX M4851-050 obtained for a $2\,K\,min^{-1}$ cooling rate in 15 µm thick cells with planar boundary conditions. Note the appearance of a smectic twist state between the cholesteric and the conventional SmA* phase for the samples doped by bent-core molecules, which is absent for the neat FLC mixture.

observe this in the bent-core or the chiral doped systems. Cooling through a biphasic region, one would expect to observe an increasing volume fraction of the low temperature phase at decreasing temperature. This is not what we observed in the investigated materials, apart from the isotropic to cholesteric transition. We can of course not conclusively exclude the existence of a very narrow biphasic region at the cholesteric to smectic transition, which may enhance the formation of TGB-like smectic ordering. Nevertheless, this should not detract from the fact that the reported twist state is for the first time reported for an achiral bent-core doped system.

It is also worth noting that the occurrence of the twist state is suppressed in very thin sandwich cells of thickness 4 µm, even on cooling. A texture photograph of the novel state is shown in figure 2 for the 2.5% HXVIII in FELIX M4851-050 mixture, cooled at $5\,K\,min^{-1}$ and confined to a relatively thick cell of gap 25 µm with planar anchoring conditions. The observed texture shows many similarities to natural textures of conventional twist grain boundary phases, such as the somewhat blurry appearance for long pitch materials under planar boundary conditions [9], and is equivalent to the twist state reported in [16], which was obtained by doping an achiral liquid crystal mixture with a highly chiral dopant.

The stability of the twist state at constant cooling rate increases with increasing dopant concentration (figure 1). It is important to note, that the smectic twist state can only be observed on cooling, i.e. in a sequence I–N*–twist state–SmA*–SmC*–Cr. On heating, the samples exhibited a sequence: Cr–SmC*–SmA*–N_∞*–N*–I, where N_∞* denotes a chiral nematic structure with infinite pitch. This behaviour is clearly illustrated by the texture photographs of 2.5% HXVIII in FELIX M4851-050 (15 µm cell) shown in figure 3, where the top row of images (*a–c*) represents the cooling cycle, while the bottom row figures 3 (*d*)–(*f*) depicts textures on heating. Figure 3 (*a*) shows a long pitch cholesteric phase in Grandjean orientation, which cannot be brought into extinction position, indicating its helical superstructure. On cooling, clear indications of smectic layering develop, as signified by the striation observed

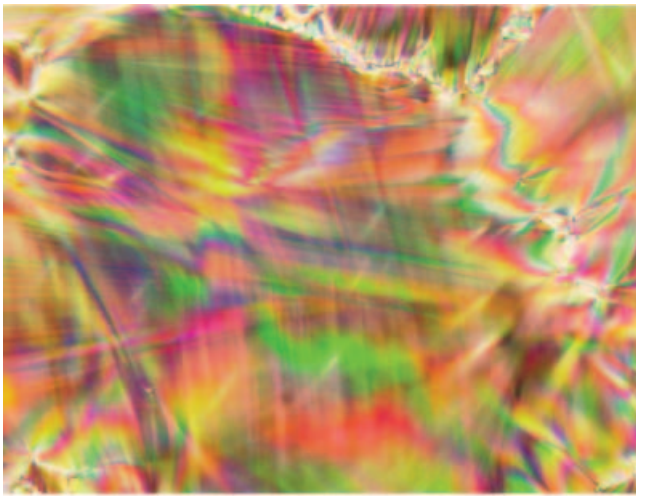

Figure 2. A typical texture photograph of the observed smectic twist state, here depicted for 2.5% HXVIII in FELIX M4851-050 in a relatively thick cell of 25 µm.

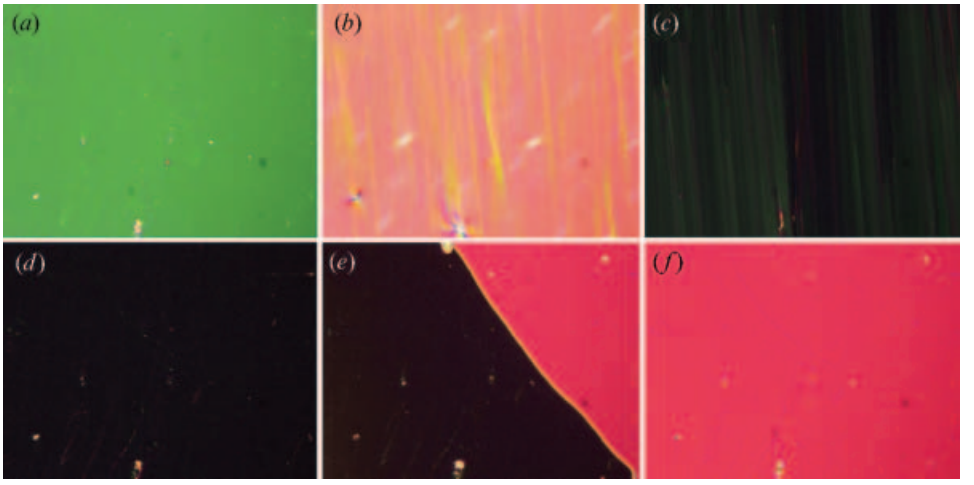

Figure 3. A typical texture series, here displayed for HXVIII-doped FELIX M4851-050 at a concentration of 2.5 wt % in a 15 µm cell with planar boundary conditions. The top row (*a*)–(*c*) shows the cooling cycle with (*a*) the cholesteric phase, (*b*) the smectic twist state and (*c*) the ordinary SmA* phase. The bottom row (*d*)–(*f*) shows the respective heating sequence from the uniform SmA* phase with (*d*) the nematic director configuration (N_∞*), (*e*) growth of the twisted cholesteric state into N_∞* until in (*f*) the whole texture is N* (see text).

in figure 3 (*b*) and the absence of the nematic 'shimmering', caused by Brownian motion [9]. The texture of figure 3 (*b*) shows slight variations in transmitted intensity when rotated between crossed polarizers, but no extinction can be observed. Further cooling results in the growth of the ordinary SmA* phase, figure 3 (*c*), which in contrast to the twisted smectic state can now be brought to extinction, while slight striations along the smectic layer normal are still observed (director along one of the polarizer directions). Interestingly, the heating process exhibits a different behaviour. Figure 3 (*d*) shows a nematic director configuration (N_∞*) which develops from the uniform bookshelf texture of the SmA* phase, figure 3 (*c*), on heating. It can be brought to extinction by rotating between crossed polarizers and exhibits the typical nematic 'shimmering', with no striations observed. Further heating results in the growth of the twisted cholesteric phase, figure 3 (*e*) top right, from the uniform chiral nematic state, bottom left, until the whole field of view exhibits a cholesteric Grandjean texture, which cannot be brought to extinction, figure 3 (*f*).

Quantitative evidence for the existence of a twisted smectic structure mediating the cholesteric and the SmA* phase is provided by optical transmission measurements as a function of cell rotation angle ϕ between crossed polarizers for the different phases involved (figure 4). In the isotropic phase (squares) the reduced transmission is obviously close to zero, independent of sample orientation. The planar Grandjean orientation of the cholesteric phase (circles) is naturally birefringent so that a transmission between crossed polarizers is observed. This is also independent of sample orientation due to the helical structure of the N* phase with the helical axis parallel to the direction of light propagation. For the conventional SmA* phase (down triangles) the typical $\sin^2(2\phi)$-functionality for the transmission is observed; a 90° periodicity with

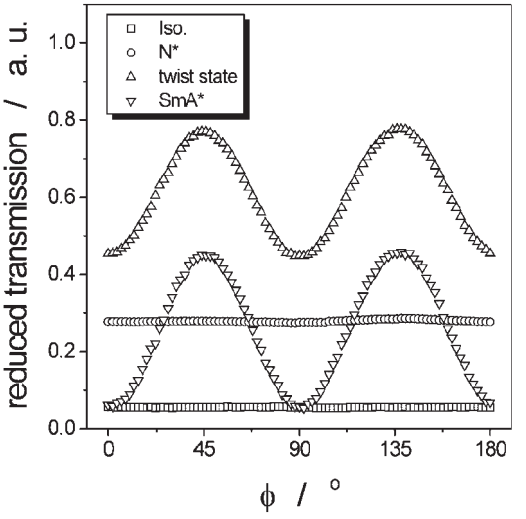

Figure 4. Reduced optical transmission as a function of cell rotation angle between crossed polarizers for the isotropic phase (squares), the cholesteric phase (circles), the smectic twist state (up triangles) and the conventional, uniformly oriented SmA* phase (down triangles). The observed intensity variation of the twist state indicates that there is no fully developed helical superstructure, while the fact that transmission does not reach the dark level of the isotropic nor the SmA* phase demonstrates the twisted nature of the intermediate state.

transmission minima whenever the director is parallel to any of the polariser directions (0°, 90°, etc.) and transmission maxima at 45°, 135°, etc. It is worth pointing out that the dark level of the SmA* transmission curve coincides with values observed for the isotropic phase, i.e. perfect extinction of the bookshelf aligned SmA* phase is observed.

The unambiguous measurements obtained from the three conventional phases I, N* and SmA* indeed support the reported smectic twist state (figure 4, up-triangles). Firstly, we note the variation in intensity with cell rotation angle ϕ, which is due to an incompletely developed helical structure (twist angle $<360°$), as compared with a fully developed helical superstructure (several pitches; twist angles>several multiples of 360°). Secondly, and most importantly, the observed transmission curves of the twist state never come close to the minimum transmission of either the isotropic or the SmA* phase, i.e. the smectic twist state cannot be brought to extinction and thus indeed represents a twisted structure, although not a perfectly and completely developed helical superstructure, as for a cholesteric phase. Since a continuous twist of a smectic A* layered material is not allowed due to elasticity (no hard deformations for incompressible smectic layers), it has to be assumed that defects, i.e. twist grain boundaries, are incorporated in the structure of the observed state. This implies a long pitch TGB-like structure, induced by a small amount of an achiral bent-core dopant, being observed between the ordinary N* and SmA* phases. Structurally, this may well be similar to the very recently discovered 'Giant-block twist grain boundary phases' reported by Fernsler *et al.* [28].

The stability of the observed smectic twist state is enhanced by (i) increasing bent-core dopant concentration and (ii) increasing dopant bend angle (possibly also mesogenic behaviour of the bent-core dopant) (figure 1), but also by (iii) increasing cooling rate and (iv) increasing sample dimension. It is thus apparent, that the observed smectic twist state is not reached via a true thermodynamic phase transition, but rather through kinetics, a viscosity-dominated process. This is exemplified by the increase of the temperature stability interval of the smectic twist state, θ, with increasing cooling rate R, as clearly shown in figure 5 for 2.5% HXVIII in FELIX M4851-050. A qualitatively equivalent behaviour is observed for other concentrations of HXVIII, as well as those of the 859 dopant molecule and the chiral dopant R1011. The stability of the smectic twist state increases with increasing cooling rate. In the extreme case of large cell gaps (25 µm) and large cooling rates (5 K min^{-1}) the observation of the ordinary SmA* and SmC* phases can even be

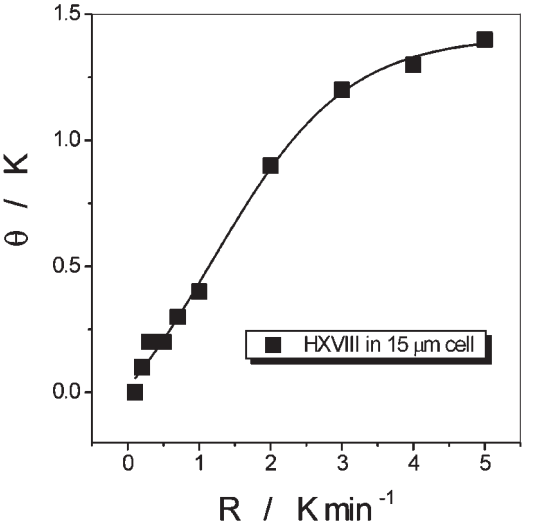

Figure 5. Dependence of the smectic twist state temperature regime of existence, θ, as a function of cooling rate R.

suppressed completely. Figure 6 captures this behaviour nicely for a texture preparation, which exhibits both the twist state (left) and the ordinary smectic phase (right) at the same time. In figure 6 (*a*) the sample is shown in the temperature regime of the SmA* phase. While the left part of the texture exhibits the twisted smectic state,

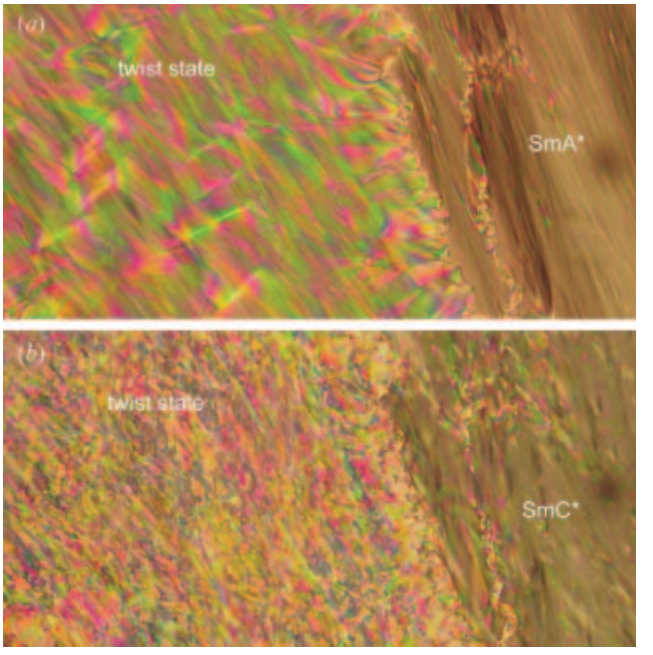

Figure 6. Textures observed for the novel twist state at large cell gaps (25 µm) and large cooling rates (R=5 K min^{-1}) in the temperature regions of the ordinary (*a*) SmA* and (*b*) SmC* phases. The left parts of the figures show the novel twist state, while the right parts display the conventional smectic textures.

the right part shows the conventional SmA* texture. Growth of this conventional SmA* texture is probably prohibited by pinning of the domain boundary. Further cooling into the temperature regime of the SmC* phase, figure 6 (*b*), results in a transition from the ordinary SmA* texture to the common SmC* texture (right). At the same time the spatial region of the twisted smectic A* structure (left) undergoes a clear transformation, while retaining its original twist. A change in texture from a first unconventional SmA* twist state to a second, unconventional SmC* twist state is clearly observed, as illustrated in the left parts of figures 6 (*a*) and (*b*).

The observations mentioned above are important with respect to the possible occurrence of a bent-core dopant-induced twist grain boundary (TGB) phase. The observed textures (figure 2) at first sight indeed suggest the formation of a TGBA* phase, promoted by the addition of achiral bent-core molecules to a chiral liquid crystal system. As exciting as this possibility appears from a fundamental physics point of view, based on the experimental results we nevertheless have to conclude that this might not be the case here. In fact, we propose that the new twist state observed in bent-core doped FLCs is not a thermodynamic phase in the conventional view, but indeed a structural smectic state exhibited under certain experimental conditions. When speaking about a thermodynamic phase, the twist state should be observed on heating as well as on cooling, which here is not the case. Possible monotropic character does not apply here, as the low temperature SmA* and SmC* phases do occur on both heating and cooling at low rates of temperature change. The preparation of samples with homeotropic boundary conditions did not result in the observation of the typical TGBA* filament texture [9].

The observed appearance and behaviour of the smectic twist state may be interpreted by several different scenarios:

(i) *The occurrence of a bent-core dopant-induced TGBA* phase*. Texture observation for planar and homeotropic boundary conditions makes this interpretation unlikely, as the samples clearly do not exhibit the expected filament textures for homeotropic anchoring. The reported smectic twist state is only observed on cooling, not on heating, which makes it unlikely to represent a thermodynamic phase transition, especially as other lower temperature transitions are not monotropic. Further, the experimentally detailed growth behaviour of SmA* domains contradicts a free energy (thermodynamic) governed behaviour, but rather suggests a kinetic, viscosity dominated growth mechanism.

(ii) *The formation of cybotactic smectic clusters* [*29*] *within the cholesteric phase*. Although we can clearly not discount cybotactic cluster formation conclusively, this would lead to a divergence of the cholesteric pitch in the vicinity of the SmA* phase [30]. This is a phenomenon that is not observed experimentally in the present systems. The latter would imply the formation of an unwound chiral nematic director configuration (N^*_∞) for the cell gaps investigated, and thus a direct transition into the SmA* phase on cooling, which is not observed. Further, the spatial dimension of cybotactic clusters is very small, orders of magnitude smaller than can be observed by light microscopy. This implies that they would not change the overall texture appearance of the cholesteric phase. Our observations, on the other hand, clearly confirm a change in texture, as shown in figure 3 (*b*).

(iii) *The formation of an induced twisted smectic, TGB-like state between the cholesteric and the uniform SmA* phase*. On cooling, the twist of the cholesteric phase is maintained, while smectic layers are formed simultaneously. This necessarily results in the introduction of defects, namely twist grain boundaries, as observed for the common TGB phase. Although forbidden in the simplest picture of smectic elasticity, it has been shown experimentally for other systems, that the layer compression modulus may indeed be strongly reduced within the vicinity of phase transitions [31, 32] (and obviously going to zero as the nematic/cholesteric phase is reached), thus favouring a twisted (probably TGB-like) director configuration. Such behaviour may be enhanced by the addition of bent-core dopants and could explain the formation and the dynamic behaviour of the observed smectic twist state formation as a hysteretic effect. The larger the cooling rate, the less the material is able to respond to the change of external conditions, in this case temperature variation. Thus, the twist state is preserved over longer times for faster cooling rates, as seen in the experiments. At the same time, the layer compression modulus increases on cooling, promoting the formation of the ordinary SmA* phase, as observed from texture studies. This latter scenario would also explain the absence of the smectic twist state on heating. Approaching the transition to the cholesteric phase on heating from the ordinary, uniform SmA* state, there is no twist to be retained and the system forms an unwound chiral nematic director configuration.

Only at higher temperatures is the cholesteric twist recovered.

Finally, we carried out quench experiments to study the growth dynamics of the SmA* phase from the smectic twist state. For each measurement, samples were heated into the isotropic phase and subsequently cooled to varying quench depths at a rate of $3\,\mathrm{K\,min^{-1}}$. Note that these investigations are different from those at constant cooling rates, as growth is observed at isothermal conditions. The quench depth ΔT denotes the difference in temperature between the twist state to SmA* texture transition recorded for very slow cooling ($0.1\,\mathrm{K\,min^{-1}}$) and the actual temperature; it thus represents supercooling of the twist state in contrast to actual twist state temperature stability. The growth of the ordinary SmA* phase is then followed under isothermal conditions. Experimental results were qualitatively equivalent for all samples investigated and exemplary data shown below is for 2.5% HXVIII in FELIX M4851-050. As a texture example, the uniformly oriented SmA* phase (dark) is observed to grow into the twist state (bright) at isothermal conditions at a quench depth of $\Delta T = 3\,\mathrm{K}$ as shown in figures 7 (*a*)–(*f*). It is interesting to note the occurrence of regular spatial interface instabilities between the uniform SmA* phase, figure 7 (*d*) bottom right, and the smectic twist state, figure 7 (*d*) top left.

For all investigations the SmA* domain boundary position changes linearly with time, as clearly quantified in figure 8 (*a*). This allows for the straightforward determination of domain boundary velocities, *v*. Figure 8 (*b*) summarizes the results obtained for the domain boundary velocity as a function of quench depth for growth perpendicular (closed squares) as well as parallel (open squares) to the smectic layer normal for a concentration of 2.5% HXVIII in FELIX M4851-050. The SmA* domain boundary velocity is found to decrease with increasing quench depth, i.e. the smectic twist state is in fact stabilized by supercooling. For very small supercooling the velocity is approximately equal in both growth directions, but as the quench depth increases, the decrease in domain boundary velocity is more pronounced in the smectic layer plane than along the layer normal. Such growth anisotropy is also observed for the formation of SmA* bâtonnets forming from the isotropic melt [9]. But in contrast to quench experiments across a first order I–LC transition, SmA* domain growth in this case is a kinetic, viscosity-dominated process, as also reflected by the quench depth behaviour. This suggests that the growth process is not related to a phase transition in the thermodynamic sense, but rather to the evolution of a non-twisted state from a twisted state. If growth were related to a true first order phase transition, the process would be dominated by the difference in free energy density ΔF between the high and the low temperature phase. ΔF strongly increases with increasing quench depth ΔT and thus implies faster growth for larger supercooling, as has been reported for several transitions, for example I–N* [33], I–SmA* [34], or even bent-core phases [35]. This is clearly not the case in the change reported here from the twisted to the uniform smectic state. Indeed the opposite behaviour is observed, which indicates that

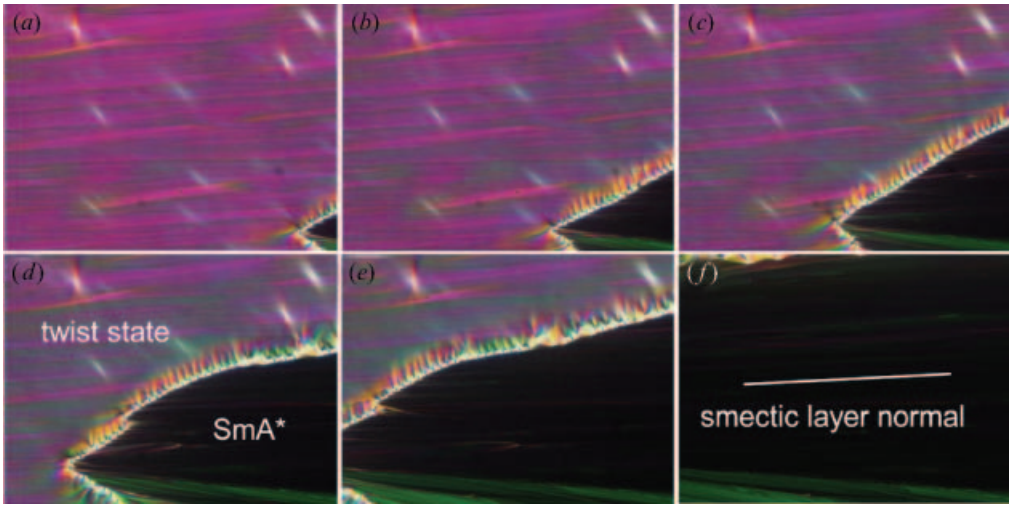

Figure 7. A typical texture series illustrating the growth of the common SmA* texture (black) into that of the smectic twist state (bright) after a temperature quench to $\Delta T = 3\,\mathrm{K}$. (*a*) $t = 40\,\mathrm{s}$, (*b*) $t = 54\,\mathrm{s}$, (*c*) $t = 68\,\mathrm{s}$, (*d*) $t = 88\,\mathrm{s}$, (*e*) $t = 108\,\mathrm{s}$ and (*f*) $t = 188\,\mathrm{s}$ after reaching isothermal conditions. Sample: 2.5% HXVIII in FELIX M4851-050, cell gap 15 µm.

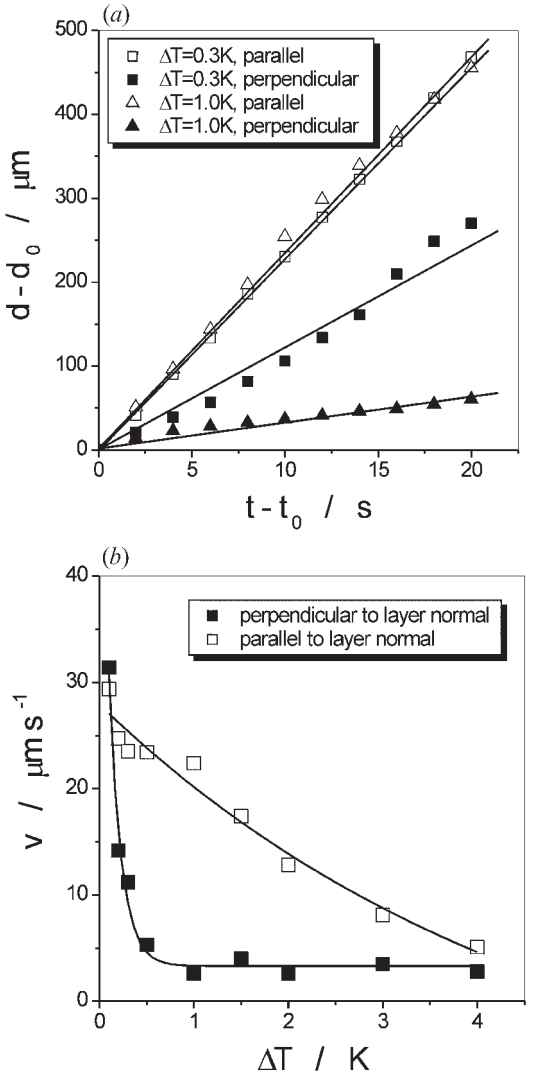

Figure 8. (*a*) SmA* domain wall position as a function of time, illustrating linear growth from the twist state both in the smectic layer plane (closed symbols) and along the smectic layer normal (open symbols) for two different quench depths. (*b*) Quench depth dependence of the domain boundary velocities for growth perpendicular (closed squares) and parallel (open squares) to the smectic layer normal. Note that the domain boundary velocity decreases for increasing quench depth, a behaviour which indicates viscosity-dominated growth in contrast to the free energy-dominated growth expected for a thermodynamic phase transition.

we are not dealing with a conventional phase transition, but rather with a structural change from a twisted to a uniform smectic A* structure, the underlying dynamics being dominated by kinetics rather than thermodynamics.

It is further noteworthy that a completely equivalent phase and physical behaviour as reported for the bent-core dopants can also be achieved by doping with a standard calamitic chiral dopant, R1011. The same textures are observed and qualitatively equivalent physical properties obtained, although the stability of the smectic twist state is somewhat more pronounced for R1011 than for the bent-core dopants. These observations signify the chiral induction capabilities of achiral bent core molecules, as previously reported as an enhancement of chirality through the study of very different properties [25–27]. We believe that the observed smectic twist structures of our present investigations represent the first stages of the formation of a bent-core dopant-induced twist grain boundary state, structurally possibly quite similar to the very recently reported GBTGB structures [28]. Unfortunately, the poor solubility of bent-core dopants in calamitic liquid crystals does not allow the observation of a true TGB phase due to phase separation at increased dopant concentrations.

4. Conclusions

The combination of the reported experimental results obtained by detailed and systematic polarizing microscopy, optical transmission and quenched growth studies, leads to the conclusion that a twisted smectic state can exist in achiral bent-core doped mixtures, observed between the cholesteric and the ordinary SmA* phase. Its occurrence is most likely related to hysteresis effects, rather than the appearance of a novel thermodynamic phase. This state is of TGB-like structure, possibly related to the very recently observed 'giant-block twist grain boundary smectic phases'. Only at lower temperatures, when the layer compression modulus is large enough to prevent a twist, does the structure change into the conventional uniform SmA* director configuration. Growth investigations suggest that the N*–twist state–SmA* sequence is a structural transition, not a phase transition in the thermodynamic sense. The studies verify the chiral induction capability of achiral bent-core molecules and show the first examples to indicate the formation of a TGBA*-like structure induced by addition of bent-core molecules to a calamitic matrix.

Acknowledgements

The authors would like to thank W. Weissflog (Halle) for providing the bent-core compounds, R. Wingen (Clariant) for supplying the FLC host and K. Tarumi (Merck) for the chiral dopant. We further thank H. Gleeson for very valuable discussions. Financial support from the Nuffield Foundation and the University of Manchester Research Support Fund is gratefully acknowledged. P.A. would like to thank the EPSRC for studentship finance.

References

[1] S.T. Lagerwall. *Ferroelectric and Antiferroelectric Liquid Crystals*, Chap. 11, Wiley-VCH, Weinheim (1999).
[2] S.R. Renn, T.C. Lubensky. *Phys. Rev. A*, **38**, 2132 (1988).
[3] J.W. Goodby, M.A. Waugh, S.M. Stein, E. Chin, R. Pindak, J.S. Patel. *Nature*, **337**, 449 (1989).
[4] J.W. Goodby, M.A. Waugh, S.M. Stein, E. Chin, R. Pindak, J.S. Patel. *J. Am. chem. Soc.*, **111**, 8119 (1989).
[5] G. Srajer, R. Pindak, M.A. Waugh, J.W. Goodby. *Phys. Rev. Lett.*, **64**, 1545 (1990).
[6] H.T. Nguyen, A. Bouchta, L. Navailles, P. Barois, N. Isaert, R.J. Twieg, A. Maaroufi, C. Destrade. *J. Phys. II*, **2**, 1889 (1992).
[7] L. Navailles, P. Barois, H.T. Nguyen. *Phys. Rev. Lett.*, **71**, 545 (1993).
[8] H.-S. Kitzerow. inH.-S. Kitzerow, C. Bahr (Eds). *Chirality in Liquid Crystals*, Chap. 10, Springer, Berlin (2001).
[9] I. Dierking. *Textures of Liquid Crystals*, Chap. 6, Wiley-VCH, Weinheim (2003).
[10] W. Kuczynski, H. Stegemeyer. *Mol. Cryst. liq. Cryst.*, **260**, 377 (1995).
[11] O.D. Lavrentovich, Y.A. Nastishin, V.I. Kulishov, Y.S. Narkevich, A.S. Tolochko. *Europhys. Lett.*, **13**, 313 (1990).
[12] S.K. Prasad, V.N. Raja, G.G. Nair, J.W. Goodby. *Mol. Cryst. liq. Cryst.*, **250**, 239 (1994).
[13] C.J. Booth, J.W. Goodby, J.P. Hardy, K.J. Toyne. *Liq. Cryst.*, **16**, 43 (1994).
[14] Y. Sah. *Mol. Cryst. liq. Cryst.*, **302**, 207 (1997).
[15] N.L. Kramarenko, V.I. Kulishov, L.A. Kutulya, G.P. Semenkova, V.P. Seminozhenko, N.I. Shkolnikova. *Liq. Cryst.*, **22**, 535 (1997).
[16] A. Chanishvili, G. Chilaya, M. Neundorf, G. Pelzl, G. Petriashvili. *Cryst. Res. Technol.*, **31**, 679 (1996).
[17] I. Dierking. *Liq. Cryst.*, **28**, 165 (2001).
[18] I. Dierking, S.T. Lagerwall. *Liq. Cryst.*, **26**, 83 (1999).
[19] J.S. Patel. *Phys. Rev. E*, **49**, R3594 (1994).
[20] T. Sekine, T. Niori, M. Sone, J. Watanabe, S.W. Choi, Y. Takanishi, H. Takezoe. *Jpn. J. appl. Phys.*, **36**, 6455 (1997).
[21] For a first review see:, G. Pelzl, S. Diele, W. Weissflog. *Adv. Mater.*, **11**, 707 (1999).
[22] D.R. Link, G. Natale, R. Shao, J.E. Maclennan, N.A. Clark, E. Körblova, D.M. Walba. *Science*, **278**, 1924 (1997).
[23] E. Gorecka, M. Nakata, J. Mieczkowski, Y. Takanishi, K. Ishikawa, J. Watanabe, H. Takezoe, S.H. Eichhorn, T.M. Swager. *Phys. Rev. Lett.*, **85**, 2526 (2000).
[24] K. Kishikawa, N. Muramatsu, S. Kohmoto, K. Yamaguchi, M. Yamamoto. *Chem. Mater.*, **15**, 3443 (2003).
[25] J. Thisayukta, H. Niwano, H. Takezoe, J. Watanabe. *J. Am. chem. Soc.*, **124**, 3354 (2002).
[26] E. Gorecka, M. Čepič, J. Mieczkowski, M. Nakata, H. Takezoe, B. Žekš. *Phys. Rev. E*, **67**, 061704 (2003).
[27] P. Archer, I. Dierking. *Phys. Rev. E*, **71**, 041713 (2005).
[28] J. Fernsler, L. Hough, R.-F. Shao, J.E. Maclennan, L. Navailles, M. Brunet, N.V. Madhusudana, O. Mondain-Monval, C. Boyer, J. Zasadzinski, J.A. Rego, D.M. Walba, N.A. Clark. In *Proc. nat. Acad. Sci. USA (PNAS)*, **102(40)**, 14191 (2005).
[29] A. de Vries. *Mol. Cryst. liq. Cryst.*, **10**, 31, 219 (1970); A. de Vries. *Mol. Cryst. liq. Cryst*., **11**, 361 (1970).
[30] R.S. Pindak, C.C. Huang, J.T. Ho. *Phys. Rev. Lett.*, **32**, 43 (1974).
[31] S. Shibahara, J. Yamamoto, Y. Takanishi, K. Ishikawa, H. Takezoe, H. Tanaka. *Phys. Rev. Lett.*, **85**, 1670 (2000).
[32] S. Shibahara, J. Yamamoto, Y. Takanishi, K. Ishikawa, H. Takezoe. *J. phys. Soc. Jpn.*, **71**, 802 (2002).
[33] I. Dierking. *J. phys. Chem. B*, **104**, 10642 (2000).
[34] I. Dierking, C. Russell. *Physica B*, **325**, 281 (2003).
[35] H.K. Chan, I. Dierking. *Phys. Rev. E*, **70**, 021703 (2004).